analytical chemistry

Article

pubs.acs.org/ac

Quantifying Synergy, Thermostability, and Targeting of Cellulolytic Enzymes and Cellulosomes with Polymerization-Based Amplification

Klara H. Malinowska, Thomas Rind, Tobias Verdorfer, Hermann E. Gaub, and Michael A. Nash*

Lehrstuhl für Angewandte Physik and Center for Nanoscience, Ludwig-Maximilians-Universität, 80799 Munich, Germany

ABSTRACT: We present a polymerization-based assay for determining the potency of cellulolytic enzyme formulations on pretreated biomass substrates. Our system relies on monitoring the autofluorescence of cellulose and measuring the attenuation of this fluorescent signal as a hydrogel consisting of poly(ethylene glycol) (PEG) polymerizes on top of the cellulose in response to glucose produced during saccharification. The one-pot method we present is label-free, rapid, highly sensitive, and requires only a single pipetting step. Using model enzyme formulations derived from *Trichoderma reesei*, *Trichoderma longibrachiatum*, *Talaromyces emersonii* and recombinant bacterial minicellulosomes from *Clostridium thermocellum*, we demonstrate the ability to differentiate enzyme performance based on differences in thermostability, cellulose-binding domain targeting, and endo/exoglucanase synergy. On the basis of its ease of use, we expect this cellulase assay platform to be applicable to enzyme screening for improved bioconversion of lignocellulosic biomass.

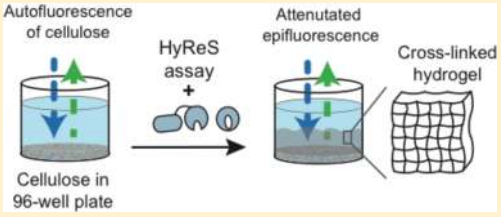

A long-standing goal in the chemical sciences has been to develop biobased systems for efficient conversion of naturally occurring plant cell wall biomass into soluble sugars. This second-generation route toward renewable fuels and chemicals has the potential to alter the international landscape governing energy and chemical commodity markets in the near future. Efficient production of soluble fermentable sugars from lignocellulosic biomass would provide a valuable input into standard fermentation processes, or alternatively feed into processes involving synthetic microorganisms for the production of a wide range of chemicals, pharmaceuticals, and other valuable products.

In order to improve biological enzyme-based conversion systems for saccharification of lignocellulosic biomass, enzyme formulations are being steadily improved through a combination of directed evolution and semirational design strategies.[1−3] In terms of screening for enzyme activity, lignocellulosic bioconversion systems present a unique challenge.[4] The lignocellulosic substrates are not easily standardized, and the mass content of the primary components (lignin, hemicelluloses, and cellulose) will vary widely depending on the nature of the feedstock, where it was grown, and how it was pretreated.[5] Also, microscopic structure of a substrate plays a key role in enzyme adsorption, kinetics, and efficiency, as shown by recent spatially and time-resolved studies utilizing fluorescence[6−9] and atomic force microscopy.[10−12] New assays for evaluating the effectiveness of enzyme formulations on real-world industrially relevant pretreated biomass that are straightforward to implement, compatible on natural substrates, rapid, and highly sensitive are therefore clearly needed.

Here we present the use of a label-free hydrogel reagent signaling system (HyReS) for assaying hydrolysis of lignocellulosic biomass. Formation of a cross-linked hydrogel at the location of glucose production attenuates the autofluorescence of cellulose and is used for quantifying total cellulolytic activity. The HyReS assay has an ability to rapidly quantify activity, thermostability, exo/endo synergy, and targeting effects in cellulotytic enzyme formulations as well as to show digestibility variations between different industrially relevant types of biomass.[13]

Assay Principle. Most of the commonly used cellulase activity assays rely on absorption or fluorescent dyes for signal detection. Those include the IUPAC-standardized colorimetric filter paper assay (FPA) in traditional[14,15] and microplate[16−18] formats, as well as bioenzymatic assays such as glucose oxidase (GOx)/horseradish peroxidase systems with fluorescence detection[19,20] and hexokinase/glucose-6-phosphate dehydrogenase systems based on nicotinamide adenine dinucleotide absorbance in the near-UV.[21,22] Novel glucose detection techniques also use fluorescent dyes for readout.[20,23−25] However, both cellulose and lignin exhibit autofluorescence,[26,27] a property that was previously used to map changes in cellulose and lignin content and their spatial distribution during biomass pretreatment[28] and to track changes in biomass structure along with localization of cellulolytic enzymes in real time.[6] As we show in this work, the intrinsic fluorescence of biomass can also be exploited to eliminate the need for dyes and labels in cellulolytic assays altogether.

Activity of cellulolytic cocktails is routinely assayed on standardized substrates such as filter paper, carboxymethyl cellulose (CMC), or Avicel[29] which, though readily available and easy to handle, have properties distinctly different from those of industrially relevant pretreated biomass.[30] The need for employing real lignocellulosic substrates in screening of cellulases is recognized in the community.[4,31,32] Several solutions have been proposed including the use of finely

Received: March 10, 2015
Accepted: June 12, 2015
Published: June 26, 2015

DOI: 10.1021/acs.analchem.5b00936
Anal. Chem. 2015, 87, 7133−7140

ground substrate in suspension[33] and preparation of substrate discs from biomass sheets.[34]

The principle of our label-free HyReS system is the attenuation of lignocellulose autofluorescence due to light scattering on a hydrogel film formed at the location of glucose production (Figure 1). The GOx/Fe(II) system, described

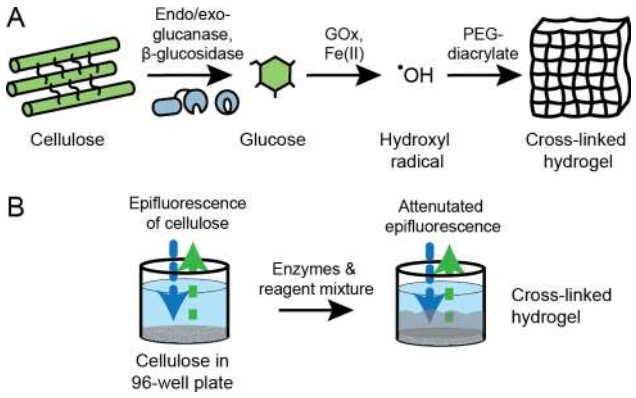

Figure 1. Schematic overview of the label-free HyReS system. (A) Cellulolytic enzymes (e.g., exo/endoglucanase and β-glucosidase) hydrolyze lignocellulosic biomass producing glucose. Saccharification products are oxidized by GOx creating hydrogen peroxide that reacts with an Fe^{2+} Fenton reagent to produce short-lived hydroxyl radicals. The hydroxyl radicals initiate free radical polymerization of a PEG hydrogel, cross-linking PEG at the surface of the cellulosic substrate. (B) Autofluorescence of cellulose in the near-UV range is used to detect the hydrogel film. Prior to hydrogel formation, the optical path between the excitation source and detector remains unobstructed and the epifluorescence signal is collected. Once glucose release initiates gel formation, both excitation and emission light is scattered by the turbid gel, resulting in signal attenuation.

previously in detail by our group and others,[25,35,36] enables selective polymerization of poly(ethylene glycol) (PEG) hydrogel in the presence of glucose. Glucose is oxidized by GOx, and the resulting hydrogen peroxide further reacts with a Fenton reagent (Fe^{2+} ions) producing ·OH radicals. The resultant hydroxyl radicals then initiate free radical polymerization of PEG diacrylate, resulting in a densely cross-linked gel. Radical polymerization serves as a signal amplification step since multiple monomers are incorporated into the hydrogel network for each released glucose molecule. The Fenton reagent can then be regenerated in the reaction of Fe^{3+} with ascorbic acid.[37] Substrate autofluorescence is measured in epi-illumination mode from above, and formation of turbid gel is detected via fluorescence signal attenuation.

RESULTS AND DISCUSSION

Substrate Characterization. We prepared 6 mm discs of pretreated biomass (napier grass and miscanthus, Figure 2, parts A and B) using standard laboratory equipment. As opposed to filter paper, pretreated biomass contains traces of lignin which influences its digestibility. Figure 2C shows Raman spectra of substrates with bands attributed to cellulose (380, 435, 1095, 1123, 1377, and 2985 cm^{-1}) present in all samples and lignin (1600 cm^{-1}) absent in filter paper.[38] Autofluorescence spectral scans of all substrates (Figure 2D–F) were dominated by broad cellulose peaks with maxima at λ_{ex} = 365 nm and λ_{em} = 430 nm.[27] An additional broad shoulder at longer wavelengths present in the spectra of napier grass and miscanthus originates from lignin,[28] while multiple bands at shorter wavelengths in the spectrum of filter paper were attributed to optical brighteners.[39] These results identify 365/430 nm wavelength as an optimal choice for universal detection of biomass substrates using the HyReS assay.

We note that drying of biomass can affect the crystalline structure and digestability. The polymerization assay, however, is also compatible with never-dried biomass. In our experience, simple centrifugation of a biomass slurry in a 96-well plate results in a compacted cellulose sediment at the bottom of the wells that is sufficiently cohesive to withstand gentle addition of liquid, allowing for the same autofluorescence measurement (described below) to be performed with never-dried biomass.

Assay Validation. In a proof-of-principle experiment, we used the label-free HyReS system to quantify cellulolytic activity of a *Trichoderma reesei* enzyme cocktail. Cellulases over a concentration range from 0 to 100 $\mu g\ mL^{-1}$ were premixed with components of the label-free HyReS assay and preheated to 37 °C. Discs of pretreated biomass were placed in wells of a microtiter plate, and the assay mix was added. The plate was incubated at 37 °C, and cellulose fluorescence was monitored over time.

The resulting time-resolved autofluorescence attenuation patterns were similar for both biomass samples (Figure 3, parts A and B, top). During the first 20 min of incubation, fluorescence intensity decreased until a plateau was reached at approximately 80% of initial signal intensity. This behavior was consistent for all wells including the negative control without cellulolytic enzymes present. This initial decrease was due to changes in the liquid meniscus shape at early time points, confirmed by time-lapse video microscopy of the wells from the side. Control measurements indicated no significant photobleaching of the sample under the experimental conditions. After this initial decline in fluorescence, a second drop in signal intensity down to approximately 40% of the initial fluorescence was observed. The second drop in autofluorescence was the result of formation of a thin, opaque hydrogel film on the substrate surface. Afterward, the fluorescence intensity rose slightly until the end of the measurement, which can be explained by a gradual evaporation of liquid from the wells, resulting in a decreased path length through the liquid.

The time at which the hydrogel film formed and attenuated the fluorescence signal was dependent on the concentration of cellulases present in the sample. Higher concentrations of cellulolytic enzymes resulted in a faster rise of glucose concentration in the vicinity of the substrate and led to earlier formation of the hydrogel film. To quantify this effect, we developed a data analysis method involving normalization, smoothing, and numerical differentiation of fluorescence time traces (see the Experimental Section). The maximum value of the derivative corresponds to the fastest signal attenuation per unit time and, consequently, to the most rapid rate of hydrogel production (Figure 3, parts A and B, bottom). The time at which the maximal signal change occurred plotted against the concentration of cellulolytic enzymes on a log scale (Figure 3C) shows that the relation between cellulose concentration and attenuation time is nonlinear. The assay is sensitive down to 3 and 1 $\mu g\ mL^{-1}$ *T. reesei* enzymatic cocktail within 200 min on napier grass and miscanthus, respectively. Longer incubation times can increase sensitivity even further. In terms of absolute glucose sensitivity, our prior work described calibration of a similar HyReS assay that did not rely on substrate

DOI: 10.1021/acs.analchem.5b00936
Anal. Chem. 2015, 87, 7133–7140

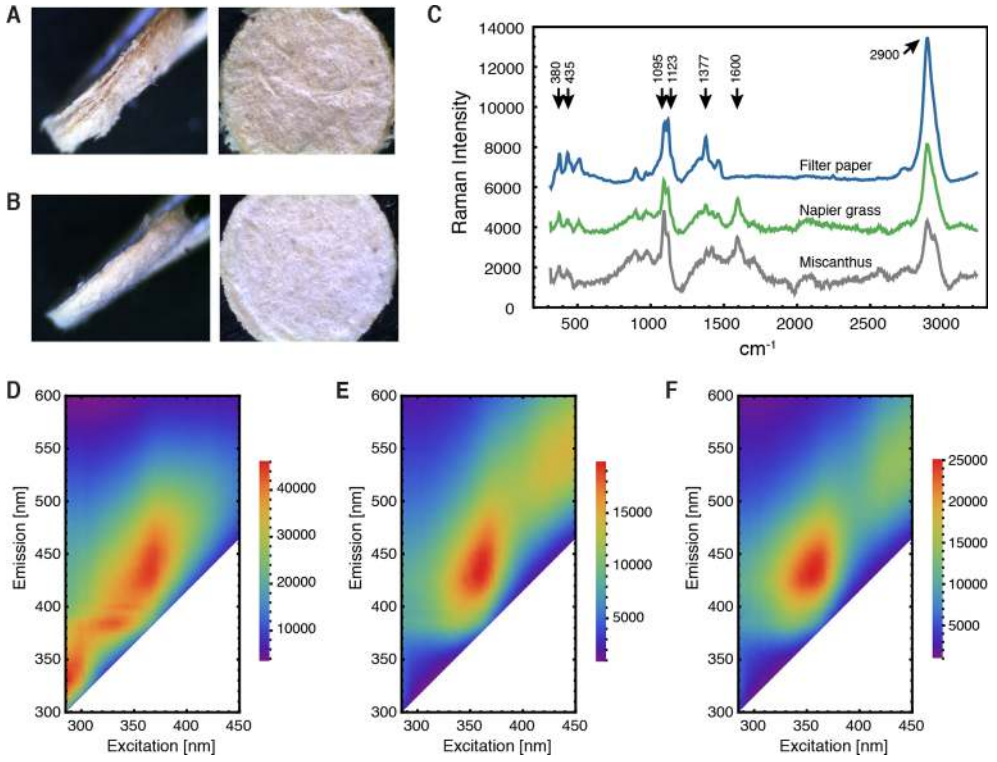

Figure 2. Pretreated biomass substrate characterization. Side and top view of cylindrical discs (6 mm in diameter) produced from (A) napier and (B) miscanthus perennial grass. (C) Raman spectra of pretreated biomass substrates using 568 nm excitation. Bands at 380, 435, 1095, 1123, 1377, and 2985 cm^{-1} were attributed to cellulose, with lignin contribution visible at 1600 cm^{-1}. Spectra were background-corrected and vertically offset for clarity. Excitation/emission autofluorescence spectral scans of (D) filter paper, (E) miscanthus, and (F) napier grass exhibited a prominent cellulose peak at ≈365/430 nm $\lambda_{ex}/\lambda_{em}$. A lignin shoulder at longer wavelengths was present in miscanthus and napier grass samples.

autofluorescence. For that system, linear dynamic range was between 0.05 and 5 mM glucose.[25]

In an analogous experiment we tested the ability of the system to detect differences in combined cellulolytic activity of exoglucanase (cellobiohydrolase I, EXG), endoglucanase (ENG), and β-glucosidase (βG) upon changes in ENG concentration. The concentrations of EXG and βG were kept constant at 1 μM and 1 mg mL^{-1}, respectively, while the concentration of ENG was varied between 0 and 0.5 μM. The position of the maximum rate of change of the fluorescence signal correlated well with enzymatic activity (Figure 4). Mixtures containing more ENG produced glucose faster and thus enabled the formation of a hydrogel film in a much shorter time.

Quantifying Synergistic and Targeting Effects. Synergy, or an enhanced activity of different types of cellulases acting together, is an important design parameter for development of multienzyme formulations.[40,41] However, synergistic effects in complex mixtures of enzymes can be hard to predict, and the extent of synergy is strongly substrate-dependent, competition being the most extreme case.[42] Also, the efficiency of targeting enzymes to the substrate by cellulose binding modules (CBMs) is strongly dependent on the microscopic structure of biomass.[43] Because of these complex enzyme−enzyme and enzyme−substrate dependencies, it is important to experimentally evaluate various cellulase compositions on relevant biomass sources to adequately judge synergy and targeting effects.

To address this point, we used the label-free HyReS assay to assess cellulolytic activity of an enzyme mixture containing 1 μM EXG, 0.1 μM ENG, and 1 mg mL^{-1} βG on miscanthus and napier grass (Figure 5). While EXG alone and combined with βG was equally effective on both substrates, the rate of glucose production from napier grass by ENG (with and without βG) was much higher than from miscanthus. As expected, combining EXG and ENG led to drastically increased hydrolysis rates on both substrates. For example, the T_{max} values for individual EXG and ENG on miscanthus were 109 and 127 min, respectively, which corresponds to the activity of approximately 4 and 1 mg mL^{-1} of *T. reesei* enzymatic mixture. The combined EXG/ENG mixture had T_{max} of 61 min, which compares with the hydrolytic potential of approximately 15 mg mL^{-1} of *T. reesei* cellulases. The activity of the EXG/ENG mixture was much higher than the sum of activities of the separate EXG and ENG enzymes independently, therefore indicating their synergistic action on solid cellulose. It is worth noting that a EXG/ENG/βG formulation was more effective on pretreated napier grass than on miscanthus, contrary to the *T. reesei* cocktail which hydrolyzed the latter substrate preferably (Figure 3).

CBMs are known to increase cellulolytic activity both when connected to single catalytic domains by flexible linkers and when incorporated into cellulosomal scaffolding.[44,45] We evaluated the effect of CBM incorporation of cellulose decomposition by comparing trimodular Cel8A-loaded mini-cellulosomes with and without a CBM in the scaffold. Concentrations of 0.2 μM of minicellulosomes (corresponding to 0.6 μM of endoglucanase) showed a significant increase in hydrolysis rate on various biomass types when loaded onto a miniscaffold containing a CBM domain (Figure 6). This was due to the high affinity of CBM to cellulose that prolonged the bound lifetime of the catalytic domains on the substrate and

DOI: 10.1021/acs.analchem.5b00936
Anal. Chem. 2015, 87, 7133−7140

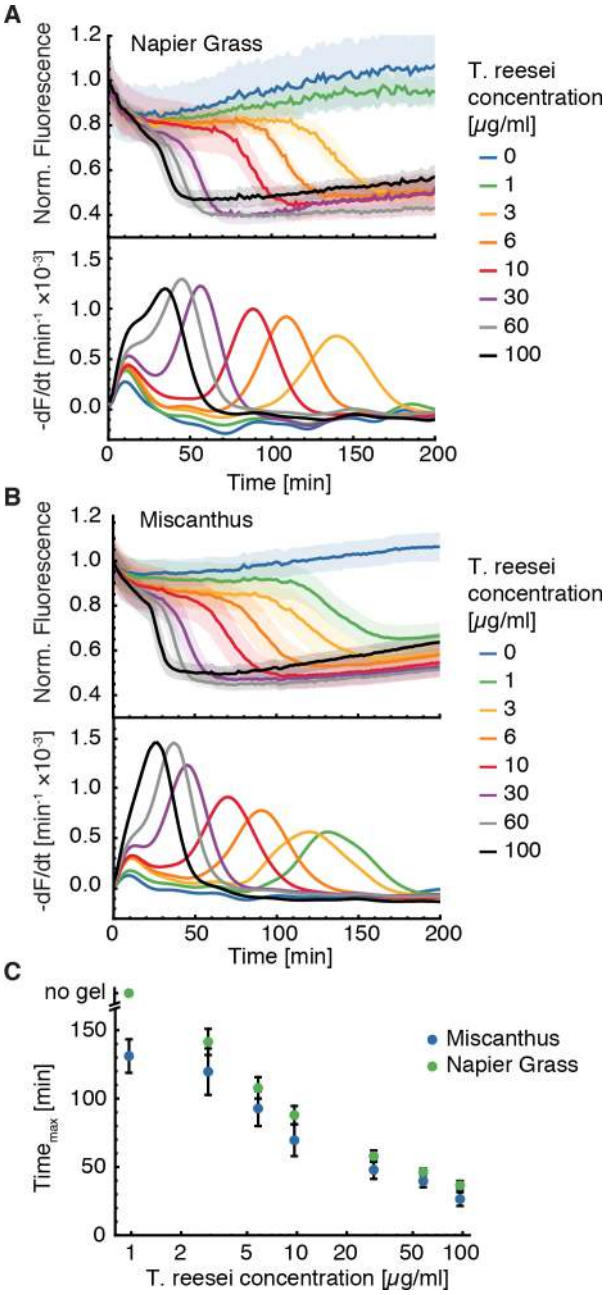

Figure 3. Detecting the cellulolytic activity of the *T. reesei* enzymatic cocktail. Attenuation of (A) napier grass and (B) miscanthus autofluorescence by the hydrogel film formed in response to enzymatic glucose production. (A and B, top) Changes of fluorescence signal in time. The shadowed area represents standard deviation of five independent measurements. (A and B, bottom) First derivative of fluorescence signal over time. (C) Time at which the peak in fluorescence derivative occurs plotted against the *T. reesei* enzymatic cocktail concentration. Lower T_{max} values represent high enzymatic activity.

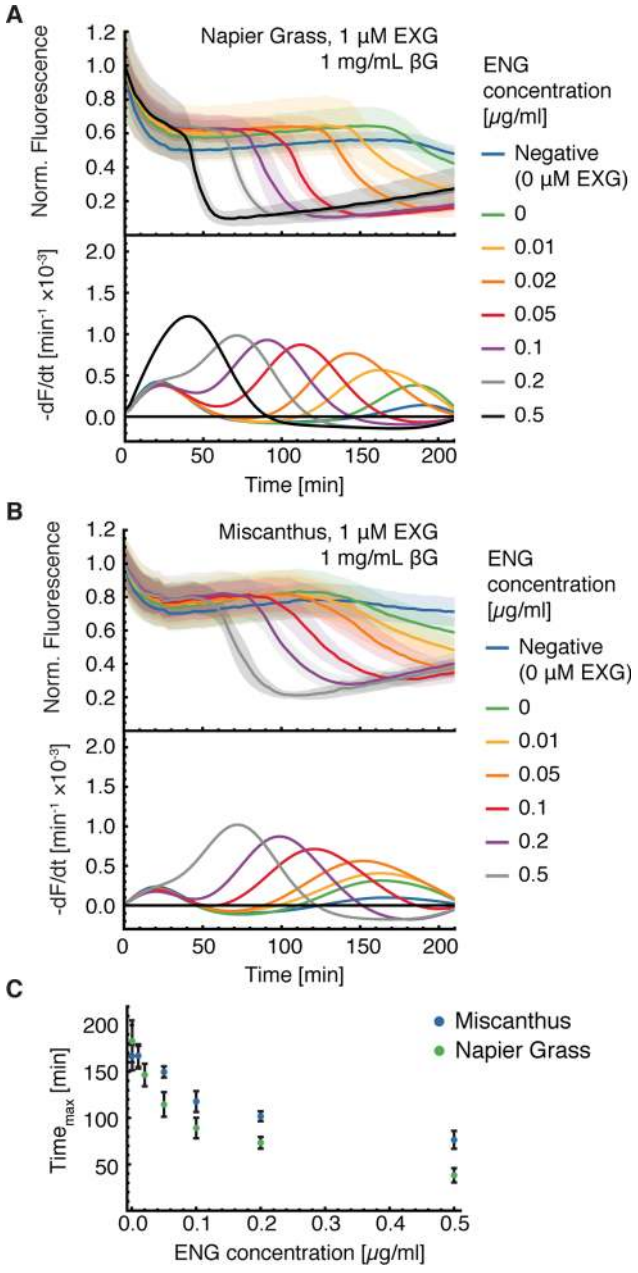

Figure 4. Detecting cellulolytic activity of an exo/endoglucanase mix by measuring attenuation of (A) napier grass and (B) miscanthus autofluorescence. (A and B, top) Changes of epifluorescent signal vs time. Shadowed areas represent the standard deviation of five measurements. (A and B, bottom) First derivative of fluorescence signal vs time. (C) Time at which the peak in fluorescence derivative occurs plotted against the ENG concentration. The concentration of EXG was kept constant at 1 μM.

increased their concentration in the immediate proximity of the substrate.

Quantifying Thermostability of Cellulases. One more application that we foresee for the HyReS assay is selecting cellulases for thermostability, a quality which can increase their lifetime under the harsh conditions required for bioprocessing.[46] As an example, two cellulases, EXG and ENG, were heat-shocked at 80 °C for variable time intervals from 0 to 90 min. Afterward, their activity on filter paper was evaluated using the dye-free HyReS assay (Figure 7). The gel formation in presence of ENG was fast regardless of prolonged heat exposure, indicating that activity of this thermophilic enzyme remained largely unaffected by temperature. On the contrary, activity of the EXG decreased drastically after 5 min of heat shock, and after 9 min gel formation was not detectable, indicating total loss of activity of this mesophilic enzyme.

DOI: 10.1021/acs.analchem.5b00936
Anal. Chem. 2015, 87, 7133−7140

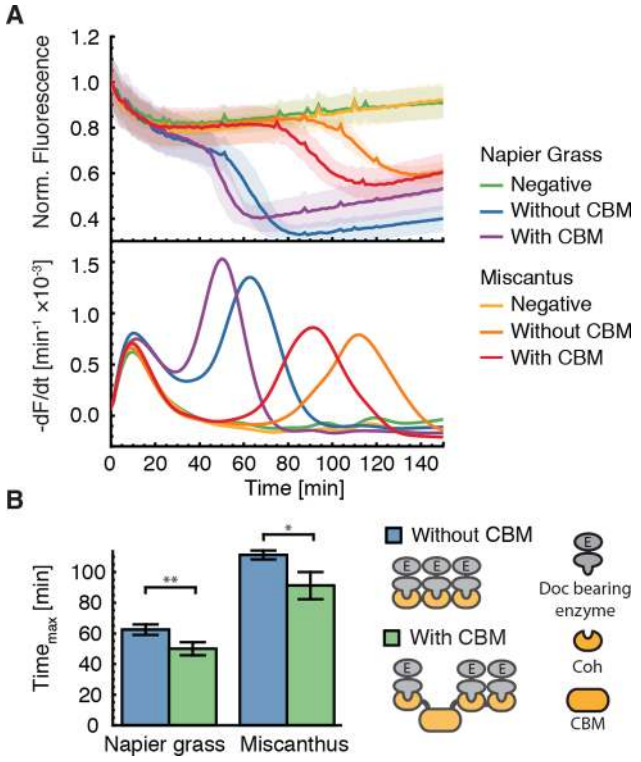

Figure 5. Activity of trimodular endoglucanase-loaded minicellulosomes on pretreated napier and miscanthus grasses. (A, top) Changes of epifluorescence signal in time. Shadow area represents standard deviation of five measurements. (A, bottom) First derivative of fluorescence signal over time. (B) Time at which the peak in fluorescence derivative occurs for miniscaffolds with and without CBM (see inset). $* P < 0.01$, $** P < 0.005$ in two-tailed unpaired Student t test.

CONCLUSIONS

Several qualities significantly differentiate the label-free HyReS system from other cellulolytic activity assays, and from our prior work.[25] The simplicity of preparation of substrate discs from virtually any type of pretreated biomass allows the assessment of hydrolytic potential of enzymatic cocktails in conditions relevant to the biomass-to-bioenergy industry. This feature circumvents the issue of many commonly used assays, including FPA, that are limited to artificial substrates.[30] Directed evolution studies would especially benefit from using natural biomass during screening processes. The screening method is of course crucial in this context. As the saying goes, "you get what you screen for".[4,47] In principle our method of preparing pretreated biomass discs can be used in combination with different sugar readout modes; however, the impact of the substrate on assay results (e.g., unspecific adsorption of dyes) should be carefully assessed.

Our label-free HyReS assay is compatible with 96-well plates allowing for easy experiment parallelization and laboratory automation. Liquid handling is relatively uninvolved, and all assay components can be premixed in bulk. After applying HyReS reagents onto biomass discs, no additional pipetting steps are required and readout takes place from the same microtiter plate. This is in contrast to the FPA and other bioenzymatic assays where the addition of further reagents and alteration of buffering conditions is necessary before developing color in an additional incubation step. The general issue of reproducibility and poor comparability due to extreme

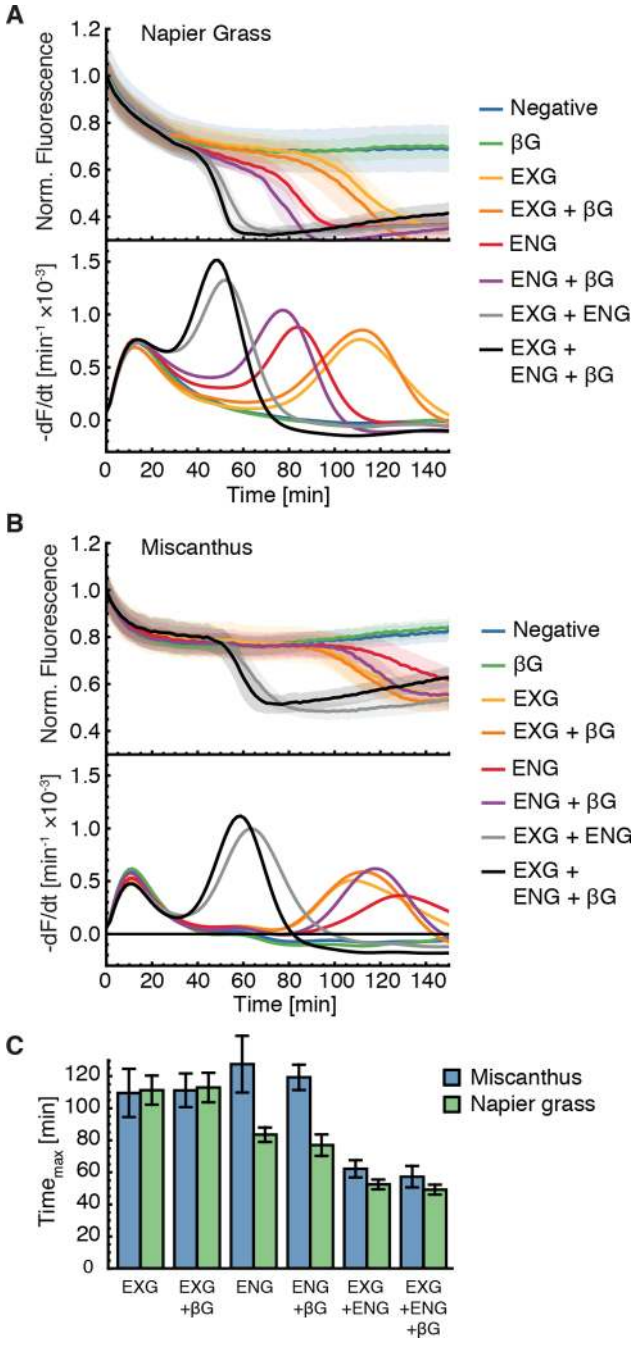

Figure 6. Detecting synergistic effects between exoglucanases (1 μM), endocellulases (0.1 μM), and β-glucosidase (1 mg mL^{-1}). (A and B, top) Changes of epifluorescence signal in time. Shadowed areas represent standard deviation of five measurements. (A and B, bottom) First derivative of fluorescence signal over time. (C) Time at which the peak in fluorescence derivative occurs for various enzyme compositions.

sensitivity to experimental conditions is a widely acknowledged problem for cellulase assays in general.[5,29] Our one-step rapid protocol simplifies the liquid handling and therefore improves reproducibility on any cellulosic substrate of choice. It is also possible to use HyReS system at elevated, more catalytically relevant temperatures (i.e., 48 °C, data not shown).

Our prior work demonstrated that the same redox/enzyme signaling pathway could be used to polymerize fluorescent hydrogels incorporating a rhodamine-acryl compound.[25] Our

DOI: 10.1021/acs.analchem.5b00936
Anal. Chem. 2015, 87, 7133−7140

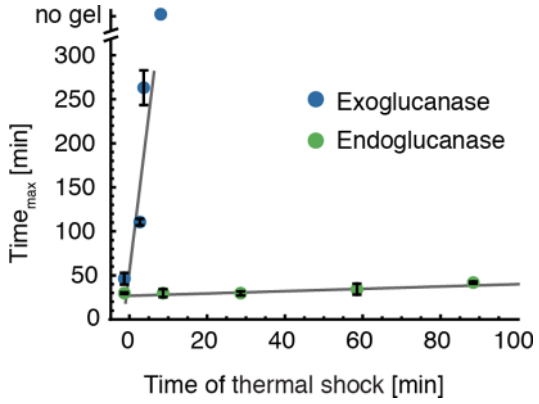

Figure 7. Thermostability of cellulases. Time needed to reach maximum of the gel growth rate is plotted against heat-shock time at 80 °C. Linear fits serve as a guide for the eye.

current method significantly differentiates itself from this prior art in several ways. First, the current method is label-free, requiring no dyes whatsoever. Instead we rely on the fluorescent emission inherent to the substrate. Second, we used here a fundamentally different measurement modality based on absorbance/scattering of excitation and emission beams, with a reflective component to the signal contributing in epi-illumination. And third, we have demonstrated for the first time the implementation of a hydrogel-based assay for differentiation of cellulase mixtures based on endo/exo synergy and CBM-targeting ability. Additionally we assayed thermostability of enzymes with the one-pot polymerization assay.

We note the assay as implemented here is primarily a threshold measurement, meaning a certain amount of glucose is required to initiate polymerization. Once the amount of glucose has been produced, polymerization occurs quickly and concludes with relatively little continued gel growth at longer time points. We took as the assay figure of merit the time required to initiate polymerization and found this to be a semiquantitative estimator of hydrolytic enzyme activity.

Despite its advantages, the HyReS system also has some associated limitations. Our one-step protocol introduces possible interference of assay components on cellulolytic activity. In particular, changes in substrate structure and enzyme−substrate interactions induced by PEG40[50] could be of potential concern. However, PEG has been shown to enhance enzymatic hydrolysis of lignocellulose, and we do not expect it to adversely affect most cellulase enzymes.[5,48,49] Potential restrictions on the HyReS assay in terms of pH requirements along with absolute glucose sensitivity are discussed in detail in our previous work.[25]

We also note that due to the complex multistep signal amplification mechanism, the response of our label-free HyReS assay is nonlinear (see Figure 3A). We believe the assay is best suited for determining early stage hydrolytic efficacy, before trapping of enzymes inside the gel structure and transport limitations become dominant. The HyReS assay cannot provide an activity measure in terms of glucose production per unit of time. It is most suitable for applications where direct comparisons between cellulolytic activities at early time points is preferred. However, we do not see this as compromising the assay applicability. Complex synergistic relationships between cellulases and an intricate interplay between substrate structure and enzyme composition limits the predictive power of rational design for enzymatic cocktails. In most cases a direct comparative empirical approach is indeed necessary.[4]

In conclusion we developed a label-free, polymerization-based HyReS for determining the hydrolysis of lignocellulosic biomass. Through radical polymerization of a cross-linked hydrogel at the location of glucose production, we achieve high signal amplification and specificity for quantifying total cellulolytic activity. Our assay is fast, easy to automate and parallelize, and can be used in combination with arbitrary (ligno)cellulose sources including pretreated biomass. The ability to determine cellulolytic activity, thermostability, exo/endo synergy, and targeting effects in cellulolytic enzyme formulations and cellulosomes establishes the HyReS assay as a valuable method for enzyme screening for improved bioconversion of lignocellulose.

EXPERIMENTAL SECTION

Materials. Exoglucanase (EXG, cellobiohydrolase I from *Trichoderma longibrachiatum*, specific activity 0.1 U/mg at 40 °C, pH 4.5) and endoglucanase (ENG, endo-1,4-β-D-glucanase from *Talaromyces emersonii*, specific activity 64 U/mg at 40 °C, pH 4.5) were purchased from Megazyme (Ireland). Cellulase from *Trichoderma reesei* ATCC 26921 (8 U/mg at 37 °C, pH 5), GOx from *Aspergillus niger*, and βG from almonds (2.1 U/mg at 37 °C, pH 5.0) were purchased from Sigma-Aldrich. Minicellulosomes consisting of three dockerin-containing CelA enzymatic units (cellulase 8A from *Clostridium thermocellum*) arranged on trimodular scaffoldin were purchased from NZYtech (Portugal). Two different scaffoldins, with (3xGH8 + Coh-CBM3-Coh-Coh) and without (3xGH8 + Coh-Coh-Coh) family 3 CBM, were used. Black, flat-bottom polypropylene 96-well plates were purchased from Grenier (Bio-One). All other reagents were obtained from Sigma-Aldrich and used without further purification.

Biomass Pretreatment. Two types of energy crops, napier grass (*Pennisetum purpureum*) and miscanthus (*Miscanthus* × *giganteus*), were used as sources of biomass. Plant matter was mechanically processed to produce coarse powder. Non-cellulosic components were extracted with 0.1 M NaOH at 80 °C for 12 h with stirring. After thorough rinsing with water, the biomass sample was delignified in 0.05 M HCl at room temperature for 12 h with stirring. The sample was washed with water until neutral pH was reached. The sample was filtered through Whatman filter paper using Büchner funnel to produce an entangled pad of ∼3 mm thickness. The pad was peeled of filter paper and dried overnight at 37 °C. Discs of 6 mm were cut out from the dry, paper-like product using a hole punch.

Raman Spectroscopy. Raman spectra were obtained using T64000 triple grating Raman system (Horiba Scientific, France). The measurements were performed in air using a 568 nm argon/krypton gas laser line (Coherent) and a 100× MPlanN air objective (NA 0.9, Olympus). Spectra were calibrated with the Raman line of silicon at 520.70 cm^{-1}.

HyReS Assay. All measurements were performed in 20 mM sodium acetate (NaAc) buffer at pH 4.5. The HyReS mix supplemented with cellulolytic enzymes of interest was freshly prepared before each experiment and preheated to 37 °C. Composition of the standard reagent mixture is shown in Table 1.

A black 96-well polypropylene plate with flat bottom was first cleaned with isopropyl alcohol and washed with deionized water. The biomass discs were carefully placed at the bottom of the plate wells, and the plate was preheated to 37 °C. The wells

DOI: 10.1021/acs.analchem.5b00936
Anal. Chem. 2015, 87, 7133−7140

Table 1. Components of Label-Free HyReS Assay

component	concentration
glucose oxidase	1 mg mL^{-1}
$FeSO_4$	250 μM
ascorbic acid	250 μM
PEG diacrylate (M_n 575)	150 mg mL^{-1}
NaAc buffer, pH 4.5	20 mM

were then filled with 200 μL of HyReS components and cellulase mixture using a multipipette and the plate was put into a multiwell plate reader (Infinite M1000 Pro, Tecan). During incubation at 37 °C the fluorescence intensity was measured from the top using a time-resolved kinetic cycle. The excitation wavelength of 365 nm and emission wavelength of 430 nm were used, and 16 reads on 4 × 4 grid were performed in each well.

Data Analysis. Each experiment was performed in quintuplicate, and a mean autofluorescence $f(t)$ with standard deviation $\sigma_f(t)$ was determined. Normalized autofluorescence $F(t)$ was calculated with respect to fluorescence at the beginning of the experiment $F(t) = f(t)/f(0)$. Error bars are plotted as standard deviation of the normalized autofluorescence $\sigma_F(t)$. Prior to numerical differentiation data was smoothed using moving average function in Igor Pro software package (Wavemetrics) using box sizes $(2M + 1)$ between 20 and 200. It is important to notice that smoothed curves were only used for numerical differentiation of data. Plots showing changes of fluorescence in time in the manuscript represent original, nonsmoothed data.

The time at which a maximum in the differentiated data occurred t_{max} was used for assessing cellulolytic activity of assay enzymes. It is reported with an error σ_{tmax} calculated from $\sigma_F(t_{max})$ according to the following formula:

$$\sigma_{tmax} = \left(\frac{dF(t)}{dt}\bigg|_{t=t_{max}} \right)^{-1} \sigma_F(t_{max})$$

Thermostability Measurement. A 10 μM solution of EXG/ENG in NaAc was heat-shocked at 80 °C for up to 90 min. Afterward it was cooled to room temperature and mixed with HyReS reagents to obtain detection solutions containing 2 μM EDG. Cellulolytic activity assay was performed as described above.

AUTHOR INFORMATION

Corresponding Author

*E-mail: michael.nash@lmu.de.

Notes

The authors declare no competing financial interest.

ACKNOWLEDGMENTS

Miscanthus samples were donated by Professor Pude (Field Lab Campus Klein-Altendorf, University of Bonn). We thank Patrick Urban (Professor Feldmann, LMU Munich) for help with recording Raman spectra. The authors acknowledge funding from the EU Seventh Framework Program NMP4-SL-2013-604530 (CellulosomePlus) and the Nanosystems Initiative Munich. M.A.N. acknowledges funding from Society in Science—The Branco Weiss Fellowship administered by the Swiss Federal Institute of Technology (ETH Zurich).

REFERENCES

(1) Heinzelman, P.; Snow, C. D.; Wu, I.; Nguyen, C.; Villalobos, A.; Govindarajan, S.; Minshull, J.; Arnold, F. H. *Proc. Natl. Acad. Sci. U. S. A.* **2009**, *106*, 5610−5615.
(2) Decker, S. R.; Brunecky, R.; Tucker, M. P.; Himmel, M. E.; Selig, M. J. *Bioenergy Res.* **2009**, *2*, 179−192.
(3) Song, L.; Siguier, B.; Dumon, C.; Bozonnet, S.; O'Donohue, M. J. *Biotechnol. Biofuels* **2011**, *5*, 3−3.
(4) Zhang, Y. P.; Himmel, M. E.; Mielenz, J. R. *Biotechnol. Adv.* **2006**, *24*, 452−481.
(5) Bailey, M. J.; Biely, P.; Poutanen, K. *J. Biotechnol.* **1991**, *23*, 257−270.
(6) Luterbacher, J. S.; Moran-Mirabal, J. M.; Burkholder, E. W.; Walker, L. P. *Biotechnol. Bioeng.* **2015**, *112*, 32−42.
(7) Yang, D.; Moran-Mirabal, J. M.; Parlange, J.-Y.; Walker, L. P. *Biotechnol. Bioeng.* **2013**, *110*, 2836−2845.
(8) Paës, G. *Molecules* **2014**, *19*, 9380−9402.
(9) Ding, S.-Y.; Liu, Y. S.; Zeng, Y.; Himmel, M. E.; Baker, J. O.; Bayer, E. A. *Science* **2012**, *338*, 1055−1060.
(10) Eibinger, M.; Bubner, P.; Ganner, T.; Plank, H.; Nidetzky, B. *FEBS J.* **2013**, *281*, 275−290.
(11) Bubner, P.; Plank, H.; Nidetzky, B. *Biotechnol. Bioeng.* **2013**, *110*, 1529−1549.
(12) Santa-Maria, M.; Jeoh, T. *Biomacromolecules* **2010**, *11*, 2000−2007.
(13) Somerville, C.; Youngs, H.; Taylor, C.; Davis, S. C.; Long, S. P. *Science* **2010**, *329*, 790−792.
(14) Miller, G. L. *Anal. Chem.* **1959**, *31*, 426−428.
(15) Ghose, T. K. *Pure Appl. Chem.* **1987**, *59*, 257−268.
(16) Decker, S. R.; Adney, W. S.; Jennings, E.; Vinzant, T. B.; Himmel, M. E. *Appl. Biochem. Biotechnol.* **2003**, *105−08*, 689−703.
(17) Xiao, Z.; Storms, R.; Tsang, A. *Biotechnol. Bioeng.* **2004**, *88*, 832−837.
(18) Cianchetta, S.; Galletti, S.; Burzi, P. L.; Cerato, C. *Biotechnol. Bioeng.* **2010**, *107*, 461−468.
(19) Kongruang, S.; Bothwell, M. K.; McGuire, J.; Zhou, M.; Haugland, R. P. *Enzyme Microb. Technol.* **2003**, *32*, 539−545.
(20) Chandrasekaran, A.; Bharadwaj, R.; Park, J. I.; Sapra, R.; Adams, P. D.; Singh, A. K. *J. Proteome Res.* **2010**, *9*, 5677−5683.
(21) Wright, W. R.; Rainwater, J. C.; Tolle, L. D. *Clin. Chem.* **1971**, *17*, 1010−1015.
(22) Chundawat, S. P. S.; Balan, V.; Dale, B. E. *Biotechnol. Bioeng.* **2008**, *99*, 1281−1294.
(23) Chang, C.; Sustarich, J.; Bharadwaj, R.; Chandrasekaran, A.; Adams, P. D.; Singh, A. K. *Lab Chip* **2013**, *13*, 1817−1822.
(24) Ostafe, R.; Prodanovic, R.; Commandeur, U.; Fischer, R. *Anal. Biochem.* **2013**, *435*, 93−98.
(25) Malinowska, K.; Verdorfer, T.; Meinhold, A.; Milles, L. F.; Funk, V.; Gaub, H. E.; Nash, M. A. *ChemSusChem* **2014**, *7*, 2825−2831.
(26) Plitt, K. F.; Toner, S. D. *J. Appl. Polym. Sci.* **1961**, *5*, 534−538.
(27) Olmstead, J. A.; Gray, D. G. *J. Photochem. Photobiol., A* **1993**, *73*, 59−65.
(28) Singh, S.; Simmons, B. A.; Vogel, K. P. *Biotechnol. Bioeng.* **2009**, *104*, 68−75.
(29) Dashtban, M.; Maki, M.; Leung, K. T.; Mao, C.; Qin, W. *Crit. Rev. Biotechnol.* **2010**, *30*, 302−309.
(30) Kabel, M. A.; van der Maarel, M. J. E. C.; Klip, G.; Voragen, A. G. J.; Schols, H. A. *Biotechnol. Bioeng.* **2005**, *93*, 56−63.
(31) Dutta, S.; Wu, K. C. W. *Green Chem.* **2014**, *16*, 4615−4626.
(32) Bornscheuer, U.; Buchholz, K.; Seibel, J. *Angew. Chem., Int. Ed.* **2014**, *53*, 10876−10893.
(33) King, B. C.; Donnelly, M. K.; Bergstrom, G. C.; Walker, L. P.; Gibson, D. M. *Biotechnol. Bioeng.* **2009**, *102*, 1033−1044.
(34) Alvira, P.; Negro, M. J.; Sáez, F.; Ballesteros, M. *J. Chem. Technol. Biotechnol.* **2010**, *85*, 1291−1297.
(35) Johnson, L. M.; DeForest, C. A.; Pendurti, A.; Anseth, K. S.; Bowman, C. N. *ACS Appl. Mater. Interfaces* **2010**, *2*, 1963−1972.
(36) Pitzler, C.; Wirtz, G.; Vojcic, L.; Hiltl, S.; Böker, A.; Martinez, R.; Schwaneberg, U. *Chem. Biol.* **2014**, *21*, 1733−1742.

DOI: 10.1021/acs.analchem.5b00936
Anal. Chem. 2015, 87, 7133−7140

(37) Xu, J.; Jordan, R. B. *Inorg. Chem.* **1990**, *29*, 4180−4184.
(38) Agarwal, U. P.; Sally, R. A. *Appl. Spectrosc.* **1997**, *51*, 1648−1655.
(39) Zollinger, H. *Color Chemistry: Syntheses, Properties, and Applications of Organic Dyes and Pigments*; Wiley-VCH: Weinheim, Germany, 2003.
(40) Kostylev, M.; Wilson, D. *Biofuels* **2012**, *3*, 61−70.
(41) Murashima, K.; Kosugi, A.; Doi, R. H. *J. Bacteriol.* **2002**, *184*, 5088−5095.
(42) Andersen, N.; Johansen, K. S.; Michelsen, M.; Stenby, E. H.; Krogh, K. B. R. M.; Olsson, L. *Enzyme Microb. Technol.* **2008**, *42*, 362−370.
(43) Boraston, A. B.; Bolam, D. N.; Gilbert, H. J.; Davies, G. J. *Biochem. J.* **2004**, *382*, 769−781.
(44) Carrard, G.; Koivula, A.; Söderlund, H.; Béguin, P. *Proc. Natl. Acad. Sci. U. S. A.* **2000**, *97*, 10342−10347.
(45) Fierobe, H.-P.; Bayer, E. A.; Tardif, C.; Czjzek, M.; Mechaly, A.; Bélaïch, A.; Lamed, R.; Shoham, Y.; Bélaïch, J.-P. *J. Biol. Chem.* **2002**, *277*, 49621−49630.
(46) Blumer-Schuette, S. E.; Brown, S. D.; Sander, K. B.; Bayer, E. A.; Kataeva, I.; Zurawski, J. V.; Conway, J. M.; Adams, M. W.; Kelly, R. M. *FEMS Microbiol. Rev.* **2014**, *38*, 393−448.
(47) Schmidt-Dannert, C.; Arnold, F. H. *Trends Biotechnol.* **1999**, *17*, 135−136.
(48) Helle, S. S.; Duff, S. J. B.; Cooper, D. G. *Biotechnol. Bioeng.* **1993**, *42*, 611−617.
(49) Kumar, R.; Wyman, C. E. *Biotechnol. Bioeng.* **2009**, *102*, 1544−1557.
(50) Li, J.; Li, S.; Fan, C.; Yan, Z. *Colloids Surf. B* **2012**, *89*, 203−210.

DOI: 10.1021/acs.analchem.5b00936
Anal. Chem. 2015, 87, 7133−7140